# Modelling three-dimensional-quench cooling for alkaline-earth atoms



2003 J. Opt. B: Quantum Semiclass. Opt. 5 S183

(http://iopscience.iop.org/1464-4266/5/2/378)

INSTITUTE OF PHYSICS PUBLISHING JOURNAL OF OPTICS B: QUANTUM AND SEMICLASSICAL OPTICS

J. Opt. B: Quantum Semiclass. Opt. **5** (2003) S183–S189 PII: S1464-4266(03)55915-8

# Modelling three-dimensional-quench cooling for alkaline-earth atoms

**T E Mehlstäubler, J Keupp, A Douillet, N Rehbein, E M Rasel and W Ertmer**

Institut für Quantenoptik, Universität Hannover, Welfengarten 1, D-30167 Hannover, Germany

E-mail: mehlstaeubler@iqo.uni-hannover.de

Received 6 November 2002, in final form 18 February 2003
Published 2 April 2003
Online at stacks.iop.org/JOptB/5/S183

**Abstract**
Quench cooling is a promising technique to reach ultra-cold temperatures in alkaline-earth atoms by Doppler cooling on ultra-narrow transitions. The principles of quench cooling are derived from an effective two-level system with a linewidth adjustable by the quenching laser. A tunable linewidth reconciles the contradictory requirements of a fast cooling rate and a high velocity selectivity at high and low temperatures, respectively. In this paper, we investigate the efficiency of quench cooling in alkaline-earth systems. We present a one-dimensional analytical description of the quenching process. Cooling and trapping in three dimensions is studied with semi-classical Monte Carlo simulations. Our results for magnesium indicate a loading efficiency of up to 40% of pre-cooled atoms at 2 mK into a QuenchMOT. Final temperatures of 9 $\mu$K and an increase in phase-space density by almost five orders of magnitude are observed in the simulations.

**Keywords:** Laser cooling, quench cooling, optical frequency standard, atom trapping, alkaline-earth atoms

(Some figures in this article are in colour only in the electronic version)

## 1. Introduction

During the past decades the issue of cooling atoms efficiently to ultra-cold temperatures, ultimately leading to quantum degeneracy, has been solved for a variety of atomic species and made them particularly attractive for atomic optics [1–7]. However, for other types of atoms with non-magnetic ground states and no hyperfine structure, many of these established techniques are not applicable. A prominent example are the alkaline-earth metals that comprise promising candidates for optical frequency standards [8–10] and simple, model-like atomic systems for the study of ultra-cold collisions [11–13]. In particular, they exhibit a rich spectrum in the optical region, with both very strong dipolar transitions and very weak intercombination lines.

A technique making use of this specific transition scheme was impressively demonstrated in the case of strontium [14, 15]. The atoms were first efficiently captured on a fast transition and then, in a second stage, Doppler-cooled on a narrow line. Finally phase-space densities of 0.01 have been reached in a simple MOT configuration [15].

The high potential of a velocity-selective excitation on narrow lines, with a linewidth $\gamma$ smaller than the recoil shift, was pointed out by Wallis and Ertmer in 1989 [16]. They predicted temperatures of the order of $h\gamma$, well beyond the recoil limit. However, in the case of Ca and Mg the natural lifetimes of the metastable states, though being suited to reach ultra-cold temperatures, are too long to allow efficient cooling of the atom. For Mg the radiative decay rate is even too low to sustain the atoms against gravity ($\Gamma < 570\ \mathrm{s}^{-1}$).

In order to extend the promising technique of narrow line cooling to Ca and Mg, we suggested quenching the lifetime of the metastable state by using a second laser to couple it to a higher-lying level with a fast decay channel to the ground state [17]. The forbidden transition is artificially broadened by the quenching light field, mixing metastable and upper excited states. A similar technique has been previously applied and theoretically studied to increase the rates of sideband cooling for trapped ions [18–20]. Recently, Doppler cooling on two-photon transitions using RF quenching has been proposed for hydrogen [21]. Quenching and cooling of neutral atoms in free space has now been successfully demonstrated for

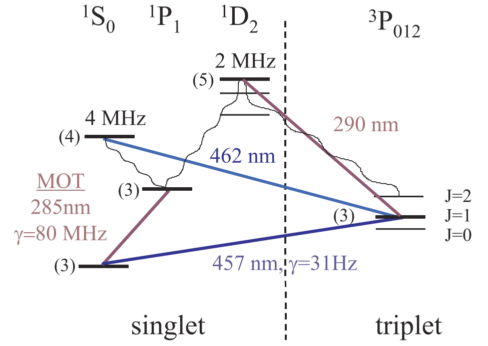


**Figure 1.** Relevant energy levels for cooling of $^{24}$Mg. The number in brackets indicates the principal quantum number. Routinely, atoms are trapped and cooled on the fast cycling transition at 285 nm. The narrow intercombination line at 457 nm between singlet and triplet systems can be used for second stage cooling. Two possible transitions for quenching are shown.

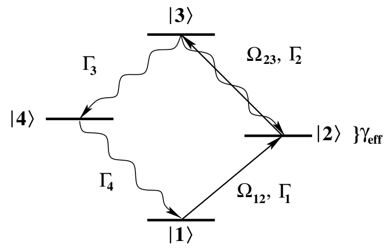


**Figure 2.** Four-level system to describe quenching in Ca and Mg. $|2\rangle$ corresponds to the metastable $^3P_1$ state, which is coupled by a second laser to a higher-lying level $|3\rangle$, with a fast decay channel $\Gamma_3$, $\Gamma_4$ to the ground state $|1\rangle$. The spontaneous decay is indicated by wavy lines. Possible candidates for the quench state $|3\rangle$ are the higher-lying $^1S_0$ or $^1D_2$ states of the singlet system.

calcium in 3D and 1D configurations [22, 23]. Its potential for sub-recoil cooling has been shown in a 1D pulsed excitation scheme [24].

In this paper we present a theoretical model for quench cooling of alkaline-earth atoms, which was used to analyse the first calcium experiments [22], and the strategy for the implementation of this scheme in magnesium. Section 2 discusses the minimum quenching rate for cooling and trapping, the choice of transition and the critical parameters with respect to Ca and Mg. In section 3 we describe the full quench cycle for a one-dimensional configuration in terms of an effective two-level system with a linewidth adjustable by the quenching laser. A full quantum mechanical treatment of the cooling cycle is given.

In the experiment atoms are simultaneously cooled and trapped in a three-dimensional MOT configuration. The two-step excitation of the quench cooling process is highly sensitive to magnetic field shifts, Doppler shifts and laser polarization. Moreover a transfer of four different recoil momenta in a single cooling cycle leads to a complex diffusion process. Therefore we have carried out three-dimensional Monte Carlo simulations based on the density-matrix formalism to investigate the efficiency of trapping and cooling in dependence on the experimental parameters. In section 4 of this paper we mainly focus on the numerical results obtained for Mg. Differences to Ca are pointed out.

## 2. Efficiency of quench cooling in alkaline-earth systems

Doppler cooling on broad lines of atoms with non-degenerate ground states is limited to the classical Doppler temperature $T_{Dopp} = \hbar\Gamma/(2k_B)$, displaying the balance between damping forces and heating due to spontaneous emissions. By cooling on the strongly coupling transitions of the singlet system (see, e.g., figure 1 for the level scheme of Mg) temperatures of the order of a few millikelvins, corresponding to a few $T_{Dopp}$, are routinely reached in magneto-optical traps for alkaline-earth atoms.

For such a pre-cooled ensemble with a mean velocity $v_{rms} \sim 1$ m s$^{-1}$ a rough estimate can be made for the cooling rate required to further slow and trap the atoms on a forbidden line. In Mg, scattering on the intercombination line 3 $^1S_0 \rightarrow 3\,^3P_1$ at 457 nm leads to a photon recoil of $\Delta v_{rec} = 3.6$ cm s$^{-1}$. Assuming a waist of $w = 2$ mm for the cooling laser and an initially pre-cooled ensemble of 1 mm diameter, scattering rates of $\Gamma_{scat} \sim 1.9 \times 10^4$ s$^{-1}$ are required to stop the atoms before they leave the interaction zone. Mainly due to its higher mass, the minimum rate on the corresponding transition in Ca is a factor of two higher. This clearly indicates the importance of artificially broadening the metastable states, which in the case of Mg and Ca have a natural radiative decay rate of only $\Gamma = 200$ and 2000 s$^{-1}$, respectively.

The effect of quenching can be derived from a simplified level scheme as shown in figure 2. The cooling laser excites the atom to the long-lived state $|2\rangle$, which again is coupled by a second laser to a higher lying state with a fast decay back to the ground state. Here $\Gamma_n$ are the natural decay rates of the transitions and $\Omega_{12}$, $\Omega_{23}$ are the Rabi frequencies for the cooling and quenching light fields, respectively. Considering the cooling cycles in steady state, the total scattering rate can be written as

$$\Gamma_{scat} = \rho_{22}\Gamma_1 + \rho_{33}\Gamma_3, \tag{1}$$

where $\rho_{22}$ and $\rho_{33}$ are the steady state populations of $|2\rangle$ and $|3\rangle$. In the limit of low saturation the population $\rho_{33}$ scales as

$$\rho_{33} \propto \frac{\Omega_{23}^2}{(\Gamma_2 + \Gamma_3)^2}, \tag{2}$$

with

$$\Omega_{23} = \frac{e}{\hbar}\langle 2|\vec{r}\cdot\vec{E}_{23}|3\rangle \propto \sqrt{\lambda_{23}^3\Gamma_2} \times |\vec{E}_{23}|. \tag{3}$$

Neglecting the weak radiative decay from the metastable state, equations (2) and (3) imply

$$\Gamma_{scat} \sim \frac{\Gamma_2 \times \Gamma_3}{(\Gamma_2 + \Gamma_3)^2} \times |\vec{E}_{23}|^2 \times \lambda_{23}^3. \tag{4}$$

The first term indicates the importance of the branching ratio $\Gamma_2/\Gamma_3$ of the upper state. The most efficient quenching is achieved when $\Gamma_2$ and $\Gamma_3$ are of the same order. In the case of alkaline-earth atoms, where the quenching state has to be coupled via a spin-forbidden transition (see figure 1), this ratio is between $10^{-3}$ and $10^{-5}$ and thus fairly high laser intensities $|\vec{E}_{23}|^2$ are required. In that respect Mg, for which the spin selection rule is stricter and branching ratios are of the order of $10^{-4}$, puts up higher demands than Ca with $\Gamma_2/\Gamma_3 \approx 10^{-3}$.

In addition, the theoretical values of matrix elements of spin-forbidden transitions in Mg and particularly in Ca bear rather large uncertainties. We have used the decay rates calculated by Kurucz [25], though recent measurements of the quenching rate in Ca for the 5 $^1D_2$ level suggest a value off by more than an order of magnitude [22]. However, new *ab initio* calculations by Derevianko and Pal'chikov [26] arrive at a similar theoretical value as Kurucz.

For the first Ca experiments, we simulated quenching on the 4 $^3P_1 \to 4\ ^1D_2$ transition with a branching ratio of $2 \times 10^{-3}$ [22]. For quench cooling of Mg we have chosen the 3 $^3P_1 \to 4\ ^1S_0$ transition at a wavelength of 462 nm, although the branching ratio of $1.3 \times 10^{-4}$ is remarkably low. Among all considered possibilities this transition is the most favourite with respect to the branching ratio, the transition wavelength and the Clebsch–Gordan coefficients. In comparison to an alternative excitation to a D level, such as the 5 $^1D_2$ state at 290 nm, the chosen transition has three clear advantages:

(1) The required power for quenching, a few 100 mW, is easier to generate in the blue spectral range.
(2) Atoms, once excited to the 4 $^1S_0$ state, cannot decay back to the triplet system through additional loss channels.
(3) In a $J = 0 \to J = 1 \to J = 0$ two-step excitation, the absorption of quenching and cooling photons coming from the same direction can be strongly enhanced, resulting in an increased cooling rate (see section 4.1).

## 3. The effective two-level system

The power of quench cooling relies on the fact that a narrow, velocity-selective transition can be tailored to efficiently trap and cool atoms at temperatures of a few millikelvins. With decreasing temperature, the quenching rate can be adapted and the ultimate high resolution of the forbidden transition reestablished. Thus one obtains the flexibility of a simple two-level system with adjustable linewidth.

Looking at equation (1) we define an effective decay rate of the metastable state:

$$\Gamma_{scat} = \rho_{22}\Gamma_{eff}, \tag{5}$$

with

$$\Gamma_{eff} = \Gamma_1 + \Gamma_3 \times \frac{\rho_{33}}{\rho_{22}}. \tag{6}$$

For small saturations and $\Gamma_2/\Gamma_3 \ll 1$ one obtains $\rho_{33} = \rho_{22}\Omega_{23}^2/\Gamma_3^2$ and

$$\Gamma_{eff} = \Gamma_1 + \frac{\Omega_{23}^2}{\Gamma_3}. \tag{7}$$

This corresponds to a tunable linewidth

$$\gamma_{eff} = \frac{\Gamma_{eff}}{2\pi} = f(\Omega_{23}^2), \tag{8}$$

which governs the velocity selectivity of the excitation. With $\Gamma_{eff}$ the excitation process can be reduced to an effective two-level system:

$$\rho_{22} = \frac{\Omega_{12}^2}{2\Omega_{12}^2 + \Gamma_{eff}^2 + 4\Delta_{12}^2}. \tag{9}$$

Equation (9) can be derived from an exact quantum mechanical treatment by adiabatically eliminating the fast decaying states $|3\rangle$ and $|4\rangle$. For the exact calculation we have solved the optical Bloch equations for the four-level system:

$$\begin{aligned} \frac{d\rho_{nn}}{dt} &= -\frac{i}{\hbar}[\hat{H}, \hat{\rho}]_{nn} \\ &\quad + \sum_k (\Gamma_{kn}\rho_{kk} - \Gamma_{nk}\rho_{nn}) \qquad \text{for } n = m, \\ \frac{d\rho_{nm}}{dt} &= -\frac{i}{\hbar}[\hat{H}, \hat{\rho}]_{nm} - \Xi_{nm}\rho_{nm} \qquad \text{for } n \neq m. \end{aligned} \tag{10}$$

Here $\Gamma_{nm}$ denotes the Einstein coefficient of transition $|n\rangle \to |m\rangle$. For the off-diagonal matrix elements the damping rate is written as

$$\Xi_{nm} = \tfrac{1}{2}\sum_k (\Gamma_{kn} + \Gamma_{km}). \tag{11}$$

The Hamiltonian $\hat{H}$ of the system consists of the unperturbed atomic energy $\hat{H}_0$ and the interaction term $\hat{V}(t)$, describing the coupling to the laser fields:

$$\hat{H} = \hat{H}_0 + \hat{V}(t). \tag{12}$$

Following [27] and using the rotating-wave approximation, a linear system for the slowly varying quantity $\sigma_{nm}$, with

$$\rho_{nm} = \sigma_{nm}(t)e^{-i\omega_{nm}t}, \tag{13}$$

can be derived for the steady state:

$$\begin{aligned} &\sum_k (\Gamma_{kn}\sigma_{kk} - \Gamma_{nk}\sigma_{nn}) \\ &\quad + \frac{i}{2}\sum_k (\Omega_{nk}\sigma_{kn} - \sigma_{nk}\Omega_{kn}) = 0, \qquad \text{for } n = m, \\ &[i(\omega_{nm} - \omega_{nm}^0) - \Xi_{nm}]\sigma_{nm} \\ &\quad + \frac{i}{2}\sum_k (\Omega_{nk}\sigma_{km} - \sigma_{nk}\Omega_{km}) = 0, \qquad \text{for } n \neq m. \end{aligned} \tag{14}$$

$\omega_{nm}^0$ is the resonant transition frequency between states $|n\rangle$ and $|m\rangle$ and $\omega_{nm}$ is the frequency of the incident laser field.

For a fixed laser power $\Omega_{12}$, the dependence of the effective scattering rate on the quench power is shown in figure 3. As an example we took the atomic parameters of Mg, where the metastable state is quenched via the 3 $^3P_1 \to 4\ ^1S_0$ transition. At low Rabi frequencies $\Omega_{23} < \Omega_{12}$, the scattering rate scales with the square of $\Omega_{23}$, as expected from equation (7). At the maximum, rates of $2 \times 10^4\ s^{-1}$ and an effective linewidth similar to the natural width of the analogous transition in Sr can be achieved. Towards higher Rabi frequencies, $\Omega_{23} > \Omega_{12}$, the increase of the effective linewidth results in a lower scattering rate, as the transition $|1\rangle \to |2\rangle$ cannot be saturated anymore. Thus $\Gamma_{scat}$ decreases as $\Omega_{12}^2/\Gamma_{eff} \propto \Omega_{23}^{-2}$.

## 4. 3D Monte Carlo simulations

### 4.1. The MOT environment

Semi-classical Monte Carlo simulations based on equation (14) extend our one-dimensional model to three-dimensional cooling and trapping in a MOT configuration. The effect of the inhomogeneous magnetic field and the changing Doppler

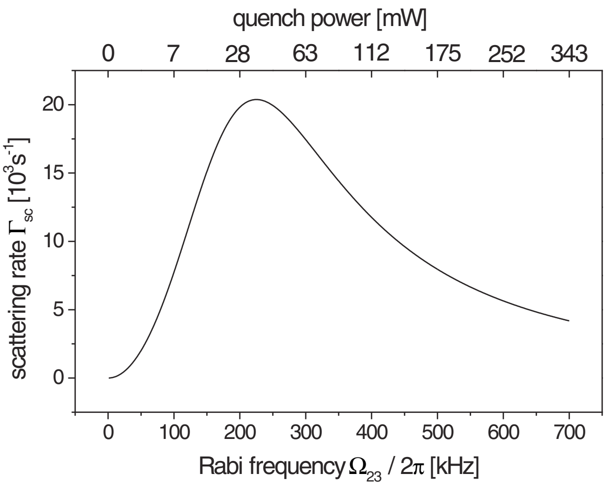


**Figure 3.** Scattering rate versus quench power for Mg. For a given $\Omega_{12}$ the scattering rate initially increases linearly with the quench power, $|\Omega_{23}|^2$. The drop-off at high power indicates a decreasing saturation of transition $|1\rangle \rightarrow |2\rangle$. Here we assume P $= 20$ mW for the cooling laser and a waist of $w_0 = 2$ mm for all laser fields.

shifts onto the narrow excitation process, and further on the complex diffusion, with four different photon recoils involved in the cooling cycle, can only be modelled numerically.

In particular, the directions of the two different recoil momenta transferred in the two-step excitation critically determine the cooling efficiency. If cooling and quenching photons are absorbed from opposite directions, the overall momentum transfer onto the atom is reduced, eventually leading to heating in the following spontaneous emission processes. In order to increase the cooling effect, both cooling and quenching recoils should add up. In the case of a $J = 0 \rightarrow J = 1 \rightarrow J = 0$ excitation, the probability of scattering from the same direction can be enhanced by choosing a $\sigma^+/\sigma^-$ molasses for the cooling beams and orthogonal polarization for the quenching beams, see figure 4. Note that, in contrast to the strict selection rules of the excitation shown in figure 4, quenching via a $J = 2$ state can only provide a selection of a polarized quenching photon, weighted by the Clebsch–Gordan coefficients of the $J = 1 \rightarrow J = 2$ transition. In that case, heating by the quenching photon can never be fully suppressed. In Mg, we follow the first scheme (quenching on the $3\,^3\mathrm{P}_1 \rightarrow 4\,^1\mathrm{S}_0$ transition) and use a QuenchMOT configuration with co-aligned cooling and quenching beams of opposite polarization[1] $\sigma^-/\sigma^+$.

For our particular excitation scheme, the Hamiltonian in the interaction frame yields eigenstates that are dark with respect to the quench excitation. However, the magnetic field of the MOT removes the degeneracy of the magnetic sublevels of the $^3\mathrm{P}_1$ state. This introduces a coupling between dark and bright states with an oscillation frequency $\omega \sim \Delta E/\hbar$, where $\Delta E$ is the energy shift between the sublevels. Even at weak magnetic field gradients of 4 G cm$^{-1}$ and an average radius of $r = 0.25$ mm these frequencies are of the order of $\omega \approx 2\pi \times 2 \times 10^5$ s$^{-1}$, faster than the typical timescales

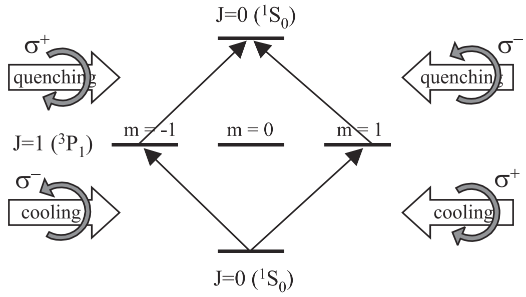


**Figure 4.** Two-step excitation for quenching via a singlet S state. For a $J = 0 \rightarrow J = 1 \rightarrow J = 0$ transition the selection rules for the angular momentum are strictest. By choosing orthogonally circular polarized light for quenching and cooling beams, one can enhance the probability of scattering both photons from the same direction.

involved in the quenching process. This allows us to use a simple semi-classical treatment in the Monte Carlo simulation.

We simulate a QuenchMOT (QMOT) with six independent laser fields each for cooling and quenching lasers. The linewidth of the quenching laser is assumed to be smaller than the linewidth of the quench state ($\gamma \approx 4$ MHz) and neglected. For the forbidden transition, the linewidth (i.e. the spectral power density) of the cooling laser critically determines the effective power driving the weak transition. In our simulations we studied the dependence on different laser lineshapes, see section 4.3. During the cooling process, the detuning of the cooling laser is varied with a rate $c$ to follow the changing Doppler shift of the slowed atoms and to optimize the trapping efficiency. The choice of initial detuning $\delta_0$ and final detuning $\delta_{end}$ determines the loading and cooling efficiency, respectively.

### *4.2. Technique*

In our simulations the classical trajectories of single atoms are traced within a time grid of 20 $\mu$s. The initial parameters of the atomic motion are generated randomly, using Gaussian distributions for the velocity with $\sigma_v = 0.81$ m s$^{-1}$ and the position with $\sigma_r = 400$ $\mu$m. At each point of the trajectory we first calculate the effective line broadening $\gamma_{eff}$ for all three magnetic substates, taking into account all contributions of the polarization states of the laser fields with respect to the local magnetic field vector, the Doppler shift and the Zeeman shift for the various transitions and light fields. This effective linewidth is convoluted with the spectral power density of the cooling laser yielding $\Omega_{12}$ for each excitation path. The excitation probabilities for all combinations of the six cooling and six quenching laser fields are calculated. For each time interval the occurrence of a cooling cycle is determined at random according to the excitation probability. In a second random process depending on the probabilities for the combinations of photon pairs, it is determined which two recoils are transferred to the atom. The momenta transferred by the two spontaneous photon recoils are chosen with isotropic distributions.

### *4.3. Results*

Starting with an ensemble of Mg atoms at $T = 2$ mK, we simulate the quenching process for $t_{cooling} = 40$ ms. A typical

[1] Compare this with the configuration in calcium, where $\sigma^-/\sigma^-$ polarization of quenching and cooling beams is chosen for quenching on a $J = 1 \rightarrow J = 2$ transition [22].

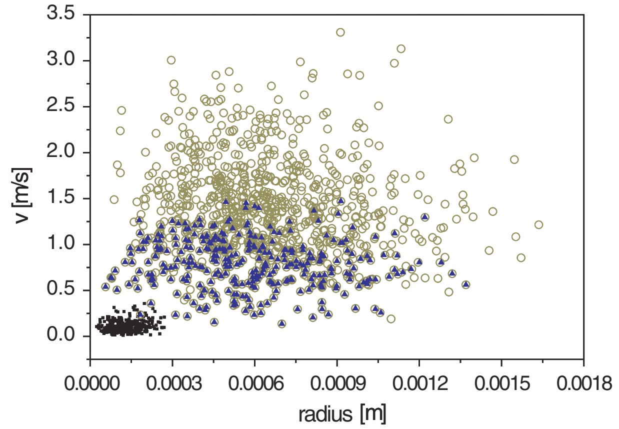


**Figure 5.** Phase-space plot of the quenching process. The cooling of 1000 atoms at 2 mK temperature (open circles) has been simulated. After 40 ms 32% of the atoms are trapped and cooled to $T = 9\ \mu$K (filled squares), resulting in an increase in phase-space density by almost five orders of magnitude. The fraction of atoms transferred to the QuenchMOT is marked with filled triangles. Parameters for the simulation were $|\nabla B| = 4$ G cm$^{-1}$, $v_0 = 1$ m s$^{-1}$, $\sigma_{laser} = 160$ kHz, $c = 80$ MHz s$^{-1}$ and $\delta_{end} = -0.64$ MHz.

phase-space plot of the cooling and trapping process is shown in figure 5. The lineshape of the cooling laser was assumed to be Gaussian with $\sigma_{laser} = 160$ kHz and the initial detuning $\delta_0$ was set to be resonant with atoms with initial velocity $v_0 = \lambda/\delta_0 = 1$ m s$^{-1}$. For a laser waist of 2 mm and a power of 20 and 30 mW for cooling and quenching beams, respectively, 32% of the pre-cooled atoms were captured in the QuenchMOT. The graph clearly shows the compression in phase space by quench cooling, resulting in an actual increase by a factor of $6 \times 10^4$. While our UV-MOT is operated at a magnetic field gradient of 130 G cm$^{-1}$, cooling rates in quench cooling are much slower and gradients of 3–4 G cm$^{-1}$ turn out to be the optimum for efficient trapping.

Whereas velocity-selective Doppler cooling takes place on the narrow transition, the detuning $\delta_{23}$ of the quench laser is best chosen to be resonant to the excited state (as the case in all the given figures). The observed loading efficiency decreases by 30% for detunings of $\delta_{23} = \pm\Gamma_3/2$. The directional selectivity of the absorbed quench photon is dominated by its polarization (cf. section 4.1).

Varying the initial detuning $\delta_0$ of the cooling laser, the simulation shows that the capture velocity, and thus the total number of atoms transferred to the QuenchMOT, is clearly restricted by the limited laser power. As seen in figure 6, atoms up to a velocity of $v_0 = 1.2$ m s$^{-1}$ can be captured by increasing the initial detuning $\delta_0$ on the cooling transition, resonant with $v_0 = \lambda/\delta_0$. This leads to a maximum transfer efficiency of 40%. Due to the limited cooling rate, however, faster atoms do not contribute to the loading efficiency. With increasing detuning, cooling of slower atoms becomes less efficient as well.

Unlike in standard cooling on broad lines, the transferred recoils of the cooling cycle shift the atom out of resonance, $\Delta\nu_{rec} > \gamma_{eff}$. Therefore the cooling process critically depends on the spectral width of the cooling laser. For our simulations for Mg we consider a Gaussian lineshape. The loading efficiency of the QuenchMOT as a function of the laser

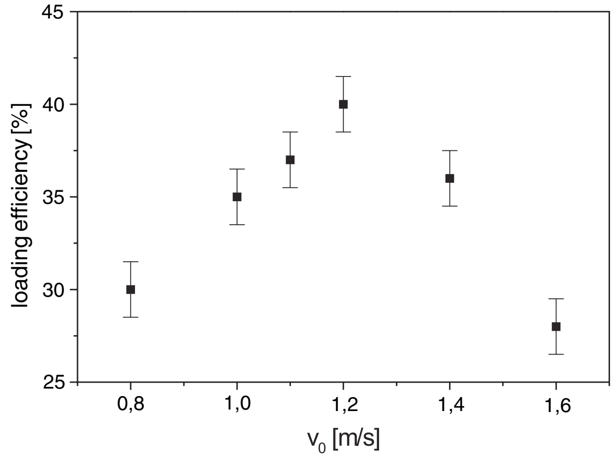


**Figure 6.** Loading efficiency versus initial detuning of the cooling laser. $v_0$ is the atomic velocity resonant at $\delta_0$. Parameters were $|\nabla B| = 4$ G cm$^{-1}$, $\sigma_{laser} = 500$ kHz, $c = 80$ MHz s$^{-1}$ and $\delta_{end} = -1.1$ MHz. The laser power was fixed at $P_{cool} = 20$ mW and $P_{quench} = 30$ mW/beam and a laser waist of 2 mm was assumed.

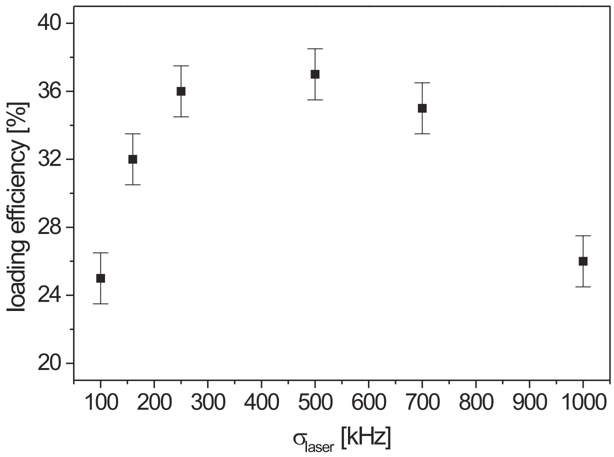


**Figure 7.** Loading efficiency with respect to the Gaussian linewidth $\sigma_{laser}$ of the cooling laser. For small $\sigma_{laser}$ atoms are lost due to spontaneous recoils, while at large $\sigma_{laser}$ the spectral power density is too low for efficient excitation on the narrow line. In the simulation we used the same set of parameters as for figure 5, but adjusted the final detuning of the cooling laser with respect to a highest loading efficiency for each $\sigma_{laser}$.

linewidth $\sigma_{laser}$ is displayed in figure 7. It shows a clear trade-off between a higher capturing probability of scattered atoms and a lower spectral power density, which in turn determines $\Omega_{12}$. With a waist of 2 mm and a laser power of 20 mW per cooling beam, a linewidth of $\sigma_{laser} = 500$ kHz turns out to be the optimum.

A different frequency profile was modelled for the quenching of Ca, where the highly stable spectroscopy laser was broadened to a rectangular profile by an AOM [22]. The steeper excitation profile of the cooling laser becomes important for quench cooling in a magnetic-field-free environment. Due to the sharp resonance, ultra-cold atoms can be collected in velocity-selective dark states, where they do not interact with the light field, and sub-recoil temperatures can be achieved [24]. For the cooling process in a MOT, the rectangular profile, as well as the Gaussian lineshape,

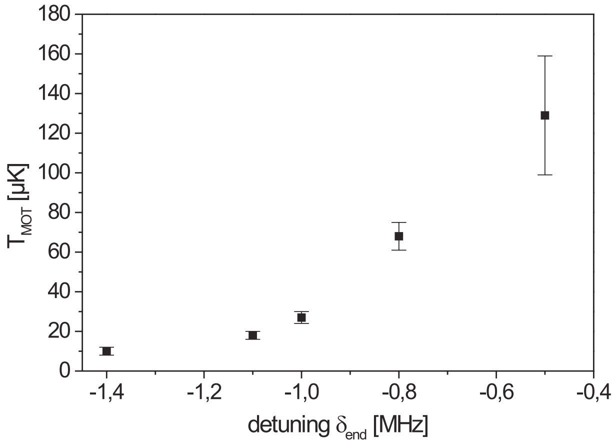


**Figure 8.** QMOT temperature versus the final detuning $\delta_{end}$. For large detunings on the cooling transition temperatures of 9 $\mu$K are observed. Apart from $\sigma_{laser} = 500$ kHz, the same set of parameters was used as for figure 5.

yield temperatures of the order of a recoil. Figure 8 shows the temperature in a QuenchMOT versus the final detuning $\delta_{end}$ of the cooling laser for magnesium. For large detuning, temperatures of 9 $\mu$K are obtained, limited by the recoil of the strong UV transition, $3\,^1P_1 \rightarrow 3\,^1S_0$.

## 5. Outlook and conclusions

In our paper we have shown that quench cooling of neutral alkaline-earth atoms in free space critically depends on the proper choice of cooling parameters and on the available laser power. In contrast to side-band cooling of trapped ions, quenching is used for both cooling and trapping of atoms within a limited interaction region. In addition, as spin-forbidden transitions are used, an unfavourable branching ratio imposes high requirements on the quench laser power.

We have shown in our calculations that the quenching rate linearly scales with the quench laser intensity (at low saturation) and with the branching ratio $\Gamma_2/\Gamma_3$. In order to account for the rather large uncertainties of *ab initio* calculations of spin-forbidden transitions, we have used the conservative estimate for the quench power of 30 mW/beam in our simulations for Mg. Nevertheless, for optimized parameters we could demonstrate a trapping efficiency of 40% of atoms pre-cooled to 2 mK. These results promise a considerable fraction of Mg atoms be transferred to a QuenchMOT. As lasers up to a few 100 mW are available in the blue spectral range, the use of a realistically higher laser power can compensate for a possible lower branching ratio.

Independent of this ratio, final QMOT temperatures of 9 $\mu$K were inferred and a linewidth of the cooling laser of 500 kHz was identified as the optimum for efficient trapping. A crucial point to obtain the best cooling efficiency is a careful alignment of cooling and quenching laser and a well-defined polarization. For the magnesium QMOT we will use overlapping beams of exact orthogonal circular polarization.

The sensitivity on a defined detuning of the quench laser and on the alignment of quenching and cooling beams was seen in the previous Ca experiment, where discrepancies between experimental and theoretical trapping efficiency of up to a factor of five have been observed [22]. According to the Clebsch–Gordon coefficients of the $4\,^3P_1 \rightarrow 4\,^1D_2$ excitation, the cooling could be enhanced with identically polarized laser beams. However, no effects of polarization have been observed, due to an imperfect alignment of cooling and quenching beams.

Comparing the quenching rates on the intercombination lines of calcium and magnesium, the latter is the experimentally more challenging element to efficiently cool and trap. Still these strongly suppressed transitions make it an excellent candidate for high precision spectroscopy. In addition, the lack of low lying D states leads to a simplest possible level scheme for collisional models. For both elements positive scattering lengths are predicted [11, 12]. Element-specific cooling techniques, such as quench cooling, can open up this way to quantum degeneracy. Heading towards this regime, Mg might prove to be a favourable candidate, as reabsorption of scattered light is strongly suppressed on its ultra-narrow line. The high potential of quench cooling to reach sub-recoil temperatures and its combination with trapping in degenerated optical dipole traps [24, 29] will reconfirm the alkaline-earth atoms in their competitive position as candidates for primary optical frequency standards.

## Acknowledgments

The authors wish to thank M Lewenstein, L Santos, U Sterr and F Riehle for valuable discussions and gratefully acknowledge co-operations with A Clairon, F Nez and F Biraben. This work has been supported by the Deutsche Forschungsgemeinschaft under SFB 407 and the European TMR Network CAUAC under HPRN-CT-2000-00165.

## References

[1] Lett P D, Watts R N, Westbrook C I, Phillips W D, Gould P L and Metcalf H J 1988 *Phys. Rev. Lett.* **61** 169
[2] Kasevich M and Chu S 1992 *Phys. Rev. Lett.* **69** 1741
[3] Aspect A, Arimondo E, Kaiser R, Vansteenkiste N and Cohen-Tannoudji C 1988 *Phys. Rev. Lett.* **61** 826
[4] Anderson M H, Ensher J R, Matthews M R, Wieman C E and Cornell E A 1995 *Science* **269** 198
[5] Davis K B, Mewes M O, Andrews M R, van Druten N J, Durfee D S, Kurn D M and Ketterle W 1995 *Phys. Rev. Lett.* **75** 3969
[6] Robert A, Sirjean O, Browaeys A, Poupard J, Nowak S, Boiron D, Westbrook C I and Aspect A 2001 *Science* **292** 461
[7] Pereira Dos Santos F, Léonard J, Wang Junmin, Barrelet C J, Perales F, Rasel E, Unnikrishnan C S, Leduc M and Cohen-Tannoudji C 2001 *Phys. Rev. Lett.* **86** 3459
[8] Oates C W, Bondu F, Fox R W and Hollberg L 1999 *Eur. Phys. J.* D **7** 449
[9] Ruschewitz F, Peng J L, Hindethür H, Schaffrath N, Sengstock K and Ertmer W 1998 *Phys. Rev. Lett.* **80** 3173
[10] Wilpers G, Degenhardt C, Binnewies T, Sterr U, Helmcke J and Riehle F 2002 *Phys. Rev. Lett.* **89** 230801
[11] Machholm M, Julienne P S and Suominen K-A 2001 *Phys. Rev.* A **64** 033425
[12] Tiesinga E, Kotochigova S and Julienne P S 2002 *Phys. Rev.* A **65** 042722
[13] Zinner G, Binnewies T, Riehle F and Tiemann E 2000 *Phys. Rev. Lett.* **85** 2292
[14] Vogel K R, Dineen T P, Gallagher A and Hall J L 1999 *IEEE Trans. Instrum. Meas.* **48** 618
[15] Katori H, Ido T, Isoya Y and Kuwata-Gonokami M 1999 *Phys. Rev. Lett.* **82** 1116

[16] Wallis H and Ertmer W 1989 *J. Opt. Soc. Am.* B **6** 2211
[17] Ly H 2000 *Diploma Thesis* Universität Hannover
[18] Dietrich F, Berquist J C, Itano W M and Wineland D J 1989 *Phys. Rev. Lett.* **42** 403
[19] Roos Ch, Zeiger Th, Rohde H, Nägerl H C, Eschner J, Leibfried D, Schmidt-Kaler F and Blatt R 1999 *Phys. Rev. Lett.* **83** 4713
[20] Marzoli I, Cirac J I, Blatt R and Zoller P 1994 *Phys. Rev.* A **49** 2771
[21] Zehnlé V and Garreau J C 2001 *Phys. Rev.* A **63** 021402
[22] Binnewies T, Wilpers G, Sterr U, Riehle F, Helmcke J, Mehlstäubler T E, Rasel E M and Ertmer W 2001 *Phys. Rev. Lett.* **87** 123002
[23] Curtis E A, Oates C W and Hollberg L 2001 *Phys. Rev.* A **64** 031403
[24] Curtis E A, Oates C W and Hollberg L 2002 *Preprint* physics/0208071
[25] Kurucz R L 1988 *Trans. IAU* **XXB** 168
[26] Derevianko A and Pal'chikov V G 2002 private communications
[27] Marquardt J H, Robinson H G and Hollberg L 1996 *J. Opt. Soc. Am.* B **13** 1384
[28] Hollberg L, Oates C W, Curtis E A, Ivanov E N, Diddams S A, Udem Th, Robinson H G, Bergquist J C, Rafac R J, Itano W M, Drullinger R E and Wineland D J 2001 *IEEE J. Quantum Electron.* **37** 1502
[29] Katori H, Ido T and Kuwata-Gonokami M 1999 *J. Phys. Soc. Japan* **68** 2479